Proceedings, 7th African Rift Geothermal Conference
Kigali, Rwanda 31st October – 2nd November 2018

Exploration of fault-related deep-circulation geothermal resources in the western branch of the East African Rift System: examples from Uganda and Tanzania

Nicholas Hinz, Bill Cumming, David Sussman

Nick.Hinz@gmail.com, *Nick.Hinz@Eager-Facility.com*

Keywords

Uganda, Tanzania, structural controls, geothermal, deep circulation, exploration

ABSTRACT

With support from the EAGER program, the geothermal exploration approach applied to prospects in the western branch of the East African Rift System (EARS) has been adopted from successful exploration and development of other global deep circulation resources. The western branch of the EARS is at an earlier evolutionary stage of continental rift development than the eastern branch, resulting in a different type of geothermal resource requiring different exploration and development strategies. Exploration in the eastern branch has identified numerous volcano-hosted, magmatically-heated geothermal resources with likely production temperatures of 200 to 350°C. In contrast, most western branch geothermal resources are heated by deep-circulation along structures that penetrate to several km depth in otherwise low permeability rocks. For these reasons the western branch resources are mostly <180°C and hosted in fractured upflows and/or lower temperature shallow sedimentary outflows. Exploration programs conducted at western rift prospects in Uganda and Tanzania since 2015 have highlighted the relevance of exploration strategies used at analogous areas in the Basin and Range region of the USA, where < 2% of the known resources are magmatically heated, that is, resources heated by emplacement of magma within 10 km from the ground surface. Exploration methods at deep circulation, fault-hosted systems are similar to those applied at volcano-hosted prospects, including the compilation and analysis of existing data, the initial prioritization of prospects based on fluid and gas geochemistry of thermal manifestations, and then detailed exploration of the higher priority areas. However, the priorities and conceptual context for subsequent data acquisition and analysis differ. For example, identifying key structural settings (e.g., fault step-overs) associated with Quaternary active fault segments and their position within the overall structural and stratigraphic framework should be given more emphasis at prospects that depend on deep-circulation in fault systems for their heat. Although resistivity methods like MT and TEM remain the most common geophysical methods used to explore deep-circulation geothermal systems, their interpretation has important conceptual differences, such as a greater focus on identifying formations that would enhance the development of fracture permeability or that might host outflow targets. Because of the relatively low level of confidence in identifying the smaller targets associated with deep-circulation zones based on surface data alone, temperature gradient wells are more often cost-effective to explore these systems than in magmatically-heated ones. During the EAGER program from 2016 through 2018, two deep circulation geothermal prospects in Uganda and one in Tanzania have been explored following these standards, supporting resource capacity assessments and recommendations for TGH drilling.

1. Introduction

The western and eastern branches of the EARS are each associated with different stages of continental rift development (Figure 1). The eastern branch of the EARS is dominated by magmatic rifting whereby axial dike intrusion and axial faulting accommodate the upper crustal extension (e.g., Morley, 1988; Ebinger and Casey, 2001; Keir et al., 2010). The axial faulting in the active magmatic rift segments has been shown to accommodate >80% of the extension in a given rift segment (Bilham et al., 1999). In contrast to the eastern branch, the western branch of the EARS is dominated by mechanical rifting with extension concentrated along border faults bounding each rift segment. Another contrast between the eastern and western branches is that the volcanic centers in the western branch are mostly fed from deep magmatic sources, with rapid ascent of magma to the surface, imparting minimal heat input to the upper crust.

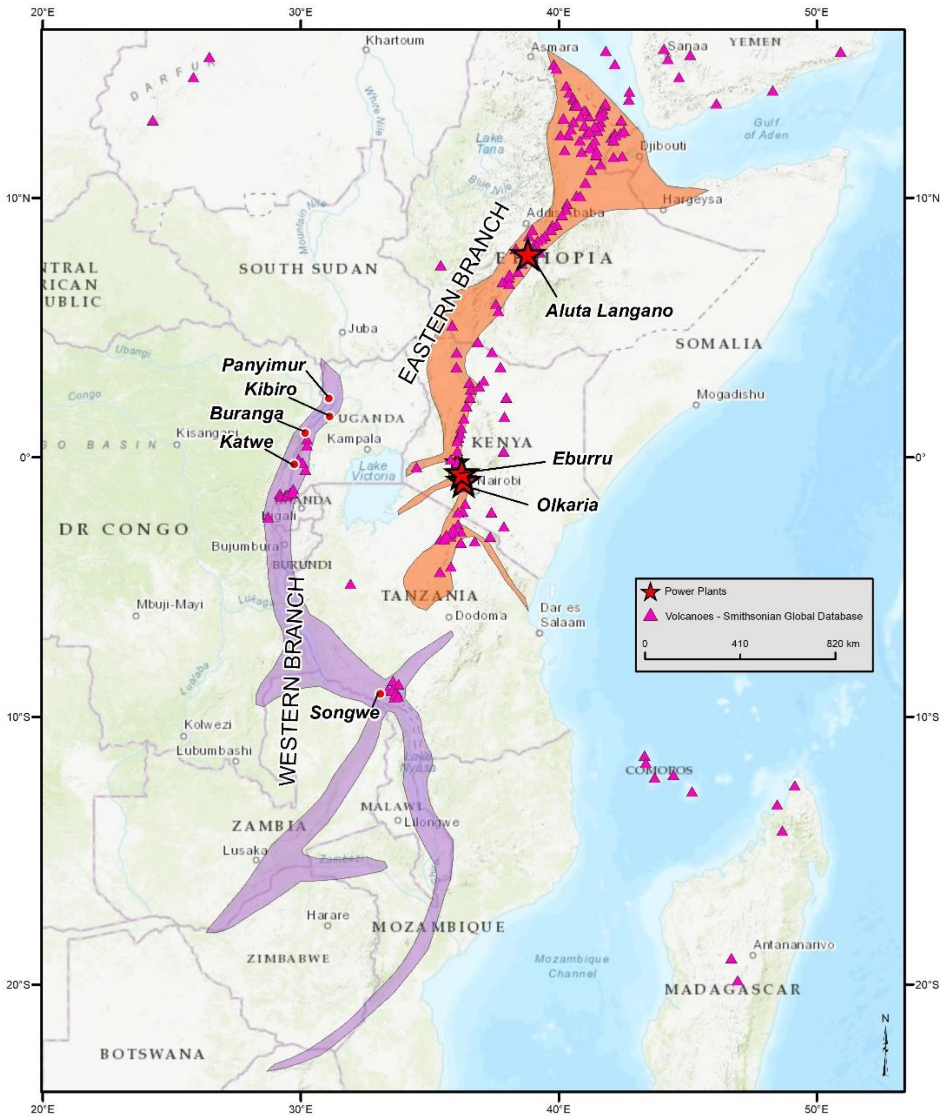

Figure 1. Eastern and western branches of the EARS (adapted from Hinz et al., 2016).

Consistent with the different types of mechanics and magmatism, the eastern and western branches are also associated with different types of geothermal resources. The eastern branch is associated with relatively abundant upper crustal magmatism and most of the geothermal resources in the eastern branch are high temperature, 230 to 350°C magmatically-heated, volcano-hosted systems (e.g., Olkaria, Kenya and Aluto-Langano, Ethiopia). Most of the known geothermal resources in the western rift are <180°C systems heated by deep circulation associated with characteristic structural settings such as fault step-overs or fault intersections (Figure 2), analogous to developed resources in the Basin and Range region, USA, and in western Turkey. Relatively few of the geothermal resources in the western branch are magmatically heated (e.g., Ngozi, Tanzania), as are < 2% of the known resources in the Basin and Range region (e.g. Long Valley; Faulds and Hinz, 2015) and arguably none of the geothermal resources in western Turkey (Faulds et al., 2009).

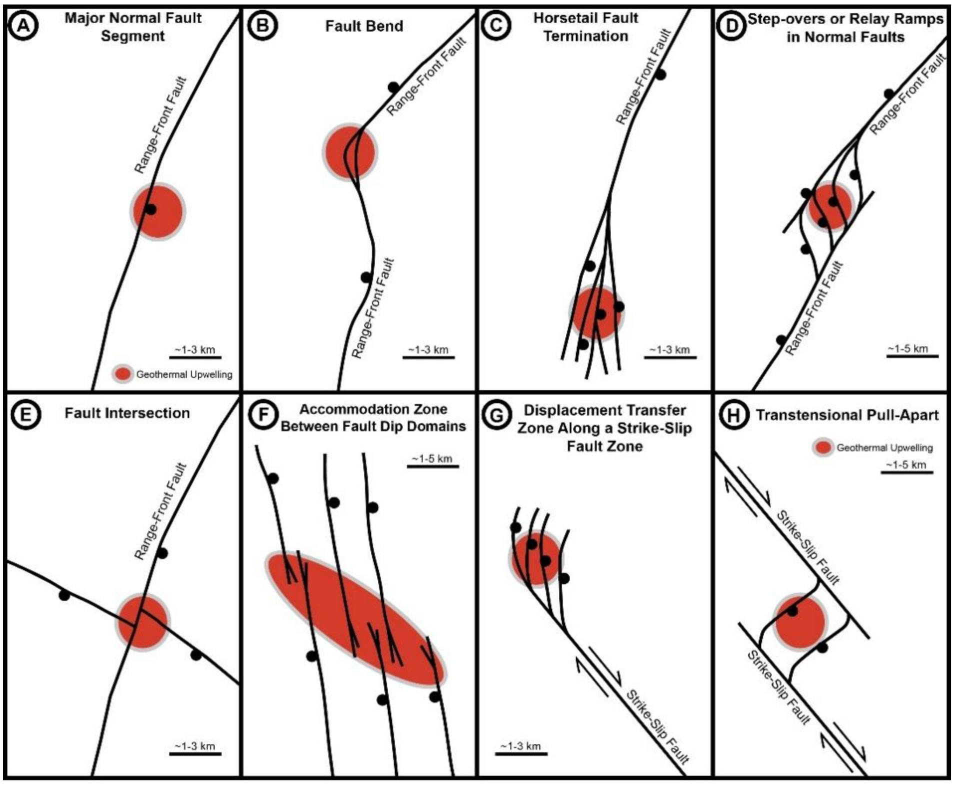

Figure 2. Structural settings of deep circulation geothermal systems in the Basin and Range region, USA (Faulds and Hinz, 2015).

Exploration methods of fault-hosted systems are similar to those applied at volcano-hosted prospects, including the compilation and analysis of existing data, the initial prioritization of prospects based on reconnaissance of fluid and gas geochemistry of thermal manifestations, and then detailed exploration of the higher priority areas. However, the priorities and conceptual context for subsequent data acquisition and analyses differ. For example, identifying key structural settings (e.g., fault step-overs) associated with Quaternary active fault segments and their position within the overall structural and stratigraphic framework should be given more emphasis at prospects that depend on deep-circulation in fault-controlled systems for their heat.

Once one or more resource areas have been prioritized for exploration and possible development, the process involves sequential steps with the interim results of each step, influencing the design and implementation of the subsequent steps. These steps include: (1) compilation and review of existing data, (2) sampling and analyzing fluid and gas geochemistry from hot springs to fill existing data gaps, (3) detailed field mapping of active and inactive surficial geothermal features, (4) detailed field mapping of the structural and stratigraphic framework, with emphasis on identifying Quaternary active fault segments, (5) selecting, designing and conducting appropriate geophysical studies based on surface geology and geochemistry, (6) developing conceptual models with all available geologic, geochemical, and geophysical data for initial work, resource capacity assessment and drill targeting, (7) targeting and implementing a temperature gradient (TG) drilling program, (8) revising the conceptual model using the TG results, and (9) given positive TG results, locating slim holes or full size wells to confirm the resource.

Three examples of this exploration process are compiled in this paper and include surface exploration studies up through targeting of TG holes. The example prospects include Panyimur and Kibiro in Uganda and Songwe in Tanzania (Figure 1). While all three prospects share a common deep-circulation theme that contrasts with the eastern branch geothermal systems, each prospect differs from each other in structural details and/or settings.

2. Panyimur, Uganda

The Panyimur geothermal prospect is located in Uganda along the northwest side of Lake Albert, in the Albertine rift segment of the western branch of the EARS (Figure 1). The Panyimur geothermal prospect was systematically explored in 2005 during a project of the Government of Uganda with technical and financial support from the World Bank and the Icelandic International Development Agency (ICEIDA). The aim of the 2005 project was to rank the geothermal prospects outside the volcanic areas of Uganda in order to prioritize their potential for detailed surface geothermal exploration (Ármannsson et al., 2007). The Geological Survey of Uganda and Mines Department (GSMD) of the Ministry of Energy and Mineral Development (MEMD) conducted geologic investigations from 2011 to 2013 in the Panyimur area (GSMD, 2012; Kato, 2013). Between 2011 and 2018, GSMD and subsequently the Geothermal Resources Department (GRD) also conducted a series of geophysical studies, including gravity and ground magnetics and, with assistance from EAGER, magnetotellurics (MT) and Transient Electromagnetic Method (TEM) surveys (EAGER, 2017a, c) and integration with existing reflection seismic and well logs from the Ondyek-1 oil exploration well located within 3 km of the prospect (Willemson et al, 2018; EAGER, 2017a). EAGER and GRD conducted additional detailed geologic mapping in 2017, with an emphasis on Cenozoic structural geology, Quaternary fault activity, and mapping and characterizing active and inactive surficial geothermal manifestations (EAGER, 2017a). The work by EAGER and GRD culminated in developing updated conceptual models and selecting targets for a TGH program based on those models (EAGER, 2017b, c).

Previous mapping identified three hot spring clusters located along the lower of two major NNE-striking fault segments bordering the Lake Albert basin near the village of Panyimur (Figure 3A). The three hot spring clusters span a 1.25 km-long segment of the lower fault and were mapped coincident with NW-striking faults intersecting the footwall side of this lower fault. The dip of the lower fault was inferred at 80° ESE.

The new geology and structural mapping confirmed that the Panyimur area is dominated by two major NNE-striking faults with normal, down-to-east displacement; both faults display Quaternary fault scarps (Figure 3B). The Upper and Lower Faults are locally linked through a left fault step, 1-2 km southwest of the three hot spring clusters. Each of these two major faults also make local and right left steps on the scale of 100 m to 600 m. The new mapping identified that the hot springs are located along relatively small step-overs along the Lower fault rather than at orthogonal fault intersections. Normal fault step-overs such as these are the most common structural setting for geothermal systems in the Basin and Range region of the USA (e.g., Faulds and Hinz, 2015).

Based on fault surface measurements in the field, the Lower Fault dips 43° to 50° ESE and the Upper Fault dips 60° to 65° ESE. The 43° to 50° dip on the Lower Fault is consistent with dip inferred by earlier GRD MT surveys and 2D inversion models supported by EAGER that corrected steeper dips inferred from a 2D seismic reflection profile. The Upper Fault offsets only Precambrian metamorphic rocks, whereas the Lower Fault offsets late Cenozoic basin-fill deposits down against the Precambrian basement by about 1500 m. The Cenozoic basin-fill consists of syntectonic lacustrine and fluvial-lacustrine sediments composed of intercalated silt, sand, and gravel. Importantly for assessing potential outflow resources in gravel in the vicinity of Panyimur, the seismic reflection profiles indicate that these sediments dip gently WSW, obliquely into the basin-bounding fault.

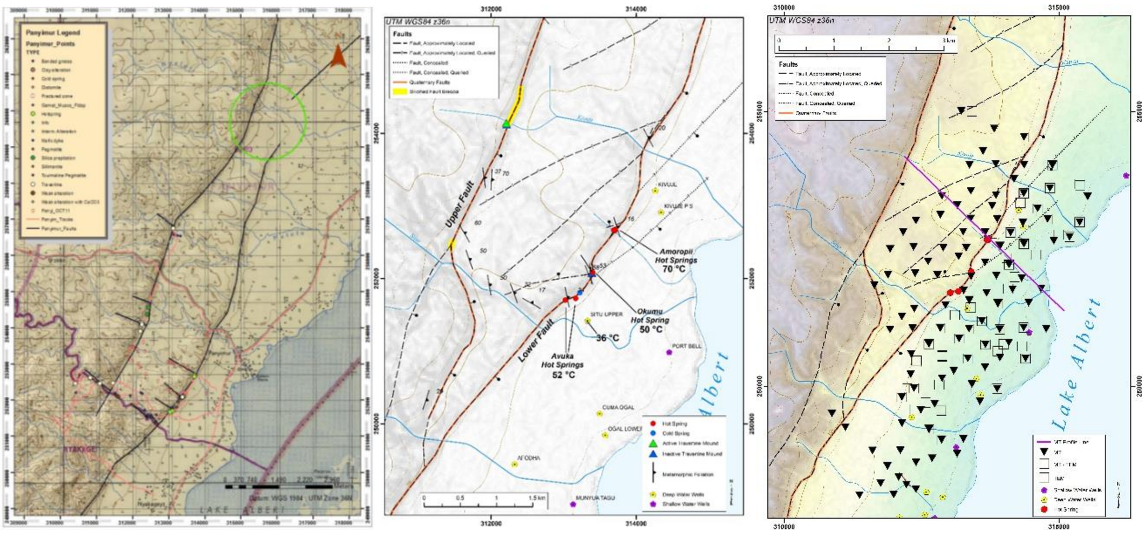

Figure 3. (A) Structural map of the Panyimur area on the left (GRD, 2012). (B) Updated map of faults and surficial geothermal features in the center (EAGER, 2017a). (C) Map of MT and TEM stations with profile location on the right.

Based on the existing geochemical data (Ármannsson et al., 2007), the Amoropii spring chemistry is consistent with an origin from a 100-120°C thermal aquifer without groundwater dilution, whereas the Okumu springs are partially diluted and the Avuka springs are mostly meteoric water. An EAGER-sponsored geochemical interpretation based on equilibration computations for locally observed minerals and for the K-Mg, chalcedony/quartz and quartz geothermometers suggest an aquifer temperature in the range of 100-120°C. Although the water chemistry provides no reliable evidence for a higher temperature, deeper aquifer, an optimistic conceptual model for Panyimur would include the possibility that the spring chemistry reflects re-equilibration in a shallow 100-120°C aquifer derived from a deeper upflow that might be as hot as 150°C based on sulphur and oxygen isotope equilibria.

The general resistivity pattern shown in the 1D TE-mode MT profiles oriented perpendicular to the strike of the Lower Fault (Figure 4) is a thick section of high resistivity to the west (deep blue to violet at the left) and a wedge of relatively low resistivity to the east (orange to red at the right) that thickens where it extends beneath the Lake Albert basin. The higher resistivity represents the Precambrian metamorphic rocks to the west of the graben boundary fault, while the lower resistivity in the basin represents a thick wedge of mainly low permeability lacustrine clay and silt intermixed with some permeable sands and gravels. Although the 2D inversion provides a more reliable estimate of the fault dip, the 1D models of the MT TE-mode are shown for the reason that they better resolve thin, low and high resistivity zones at shallow depths. The thin shallow strip of low resistivity (red) rock extending from the hot springs towards the basin is likely to consist of clays that could act as a “cap” over an eastward-verging outflow plume flowing in higher resistivity sands and gravels from an upflow hosted in permeable structures associated with the Lower Fault.

The conceptual models proposed for Panyimur include: 1) downflow and upflow in fault/fracture hosted permeability within the damage zone and fault splays directly associated with the Lower fault; 2) scenario 1 with 125°C extending to shallower depths where geothermometers re-equilibrate in a shallow outflow aquifer, implying a larger volume system; and 3) either scenarios 1 or 2 coupled to up-dip outflow in a sand or gravel formation toward the lake.

Figure 4 illustrates a cross-section showing resistivity from a 1D inversion of the MT TE-mode through the Amoropii hot spring. For a median resource conceptual model that includes upflow in a fault zone associated with the Lower Fault and modest outflow in the sediments at <85°C. Because the geochemistry of Amoropii is consistent with water coming directly from an equilibrated geothermal reservoir, the isotherm pattern in Figure 4A indicates a shallow >75°C outflow at the hot spring temperature in a >5 ohm-m (yellow), poorly consolidated sand/gravel below a <5 ohm-m (red) clay cap. A >125°C upflow is confined to the fault zone deeper than 1500 m. An optimistic resource model for Panyimur is illustrated with isotherms Figure 4B. The isotherm pattern assumes that a deep 150°C upflow ascends fracture permeability associated with the Lower Fault and outflows at 115 to 125°C in a sand/gravel aquifer at about 300 m depth, and also indirectly outflows at 75°C into a shallower and thinner sand-gravel aquifer at about 70 m depth (red arrows, Fig. 4B). The geothermometry re-equilibrates in the outflow aquifers to be consistent with the chemistry of the hot springs. The buoyant outflow aquifers thin to the southeast beneath the lake and so the MT does not resolve them but reflection seismic data shows a general dip up below the lake.

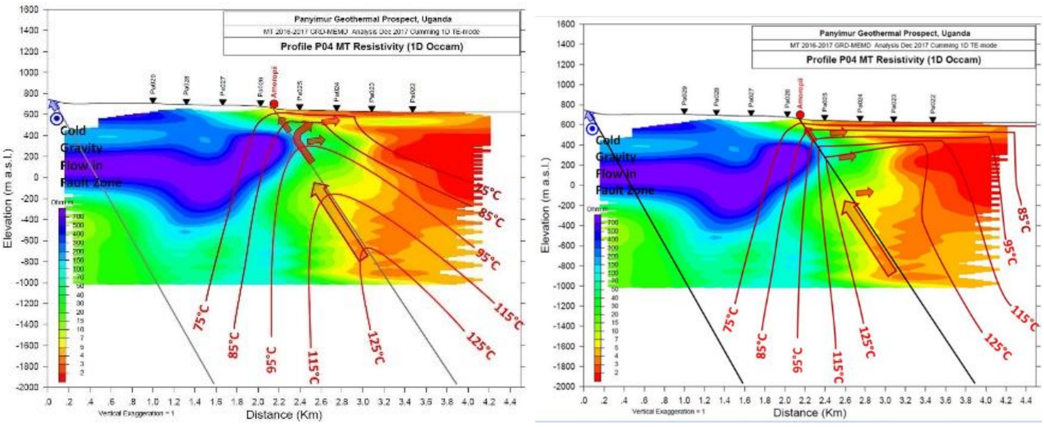

Figure 4. (A) Panyimur median case resource conceptual model through Amoropii hot spring on the left. (B) Panyimur optimistic case resource conceptual model in the center. Profile location on Figure 3C.

3. Kibiro, Uganda

The Kibiro geothermal prospect is located in Uganda along the east side of Lake Albert, on the opposite side of the Albertine Basin from Panyimur (Figure 1). Geothermal investigations at Kibiro were initiated by DGSM in 1993 with assistance from UNDP (Gíslason et al., 1994). The primary initial conclusion for this prospect, was the geothermometry indicated the presence of a 200°C reservoir temperature (Ármannsson 1994). DGSM conducted a second project from 1999 to 2002 (IAEA, 2003) and concluded that the source of recharge was meteoric water from higher ground, inland away from the rift. However, the isotope geothermometers indicated lower reservoir temperatures (140°C) than earlier cation geothermometer interpretations, and the interpretations from the isotope analyses were that the reservoir rock at Kibiro was within the Precambrian metamorphic basement. On the basis of this model, in 2004 and 2005, ICEIDA and DGSM conducted surface exploration at Kibiro to the east of the rift boundary fault, including geological mapping, a TEM resistivity survey, and gravity and magnetic surveys (Gíslason et al., 2004). The resistivity survey showed vertically distributed zones less than 300 m in width of low to very low (<1 ohm-m) resistivity in the Precambrian metamorphic rocks, which generally have very high resistivity of >5000 ohm-m. Because the isotopic study suggested that the thermal water originated from higher elevation areas to the southeast, it was assumed that the hot springs close to the Kibiro village below the fault escarpment were fed by geothermal water in the basement rock to the south or southeast of Kibiro. Based on the conclusions of the 2004-2005 surveys, six temperature gradient wells were drilled in the basement rock of the escarpment south of Kibiro. The results of the drilling showed a maximum temperature of 35°C closest to the Kibiro hot springs and low, generally conductive temperature gradients typical of other ancient continental shields (e.g. the Canadian and South African shields). Along with the conductive gradients, the different water levels in most wells indicated a general lack of permeability in the Precambrian basement, except in isolated fracture systems. The well cuttings demonstrated that the low-resistivity features in the basement rock were caused by relict conductive mineralization (Árnason & Gislason, 2009).

In 2011, the Government of Uganda decided to fund its own Uganda Geothermal Resources Development Project 1199. The UGRD program conducted geological and geophysical surveys (gravity and magnetics) at Kibiro in 2012 and 2013 (Mawejje et al., 2013; Kahwe, 2013). The focus was on the main rift fault, thermal manifestations, and mafic dykes. In contrast to the ICEIDA study, the conclusion was that upflow at Kibiro was up the main basin-bounding fault.

Following this UGRD study, MEMD/GRD was supported by UNEP-sponsored consultants in studies conducted in 2015 and 2016, including field geologic investigations, a review of the geochemistry data, a review of nearby well and reflection seismic data from Albert Basin oil exploration, a review of existing geophysics data and acquisition of new TEM and MT data, a soil gas and temperature survey, conceptual model development, and TG drill targeting (Alexander et al., 2016c). Consistent with the interpretations in the previous UGRD study, it was noted in the UNEP study (Alexander et al., 2016a) that the clusters of hot springs at Kibiro discharge through fractured rock due to the enhanced permeability of the intersection of the NTB fault and minor fault splays of the Kachuru fault. Re-analysis of the geochemistry indicated that the Kibiro hot springs were most likely associated with a 115 to 150°C fault-hosted upflow. In contrast to the previous ICEIDA study, which indicated that the deep reservoir was hosted in the Precambrian rock to the SE of Lake Albert, the UGRD and UNEP studies proposed that the deep geothermal reservoir is probably hosted in the sedimentary rocks above the pre-rift basement beneath Lake Albert. A review of the stratigraphy near shore based on oil exploration well Waki-B1 shows that a ~15 m thick conglomerate unit at the base of a sandstone interval from about 800 to 1000 m that may provide a deep sedimentary reservoir. Shallower than 800 m, shale dominates over sandstone in Waki-B1, capping the deeper reservoir. However, Waki-B1 stratigraphy may not be representative of the small deltas at and to the SE of Kibiro (Figure 6). MT and TEM resolve a low resistivity zone interpreted as a claystone with a base shallower than 300 m gently dipping up from the Kibiro hot springs toward the lake, potentially capping a thermal outflow in a sand-gravel extending below the delta at Kibiro and perhaps also to the SE as suggested by the TEM conductance in Figure 7.

EAGER and GRD conducted new detailed geology and structure mapping at Kibiro in 2018. As shown in Figure 5A, the Northern Toro Bunyoro (NTB) fault is straight. The new mapping shows that the Kibiro geothermal area is located along a complex system of fault step-overs with a combined length over 1.5 km and width of up to 150 m (EAGER, 2018a; Figure 5B). Each step is also associated with one or more fault intersections in the footwall and/or hanging-wall side. As with Panyimur, Kibiro also occupies a normal fault step-over (e.g., Figure 2).

Fault dip measurements on the upper splay of the NTB fault and the Kachuru fault are 65° NW and 46° to 50° NW, respectively. The 65° dip measurement of the upper splay of the NTB fault matches with the drill-hole data-derived 65° dip estimate on the main strand of the NTB fault north of Kibiro (Alexander et al., 2016a) and the 2D MT inversion model (Figure 6B). Quaternary scarps are associated with both strands of the NTB fault and the first 2-3 km of the Kachuru fault as it extends south from the NTB fault. Based on the distribution of fault scarps it is probable that Quaternary slip on the north end of the Kachuru fault is synchronous with slip along the NTB fault zone.

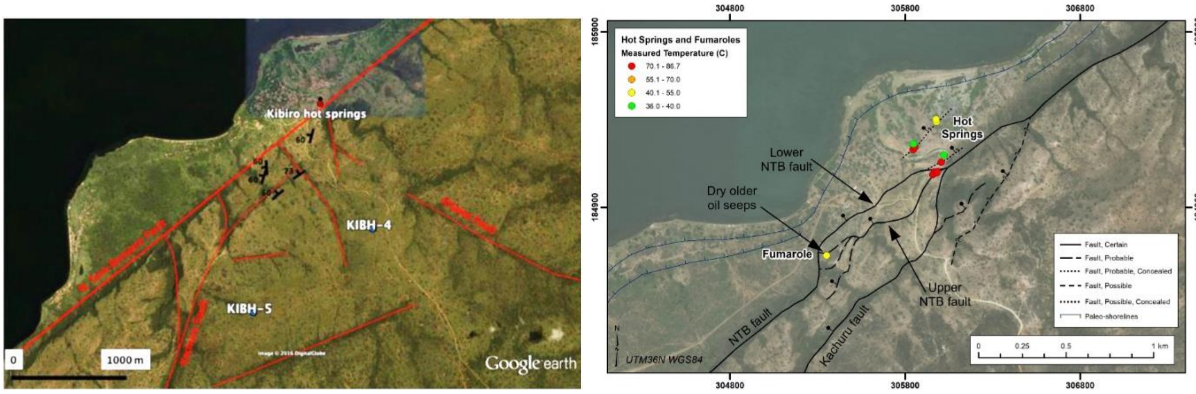

Figure 5. (A) Previous geologic map of Kibiro on left (Alexander et al., 2016a). (B) New structural geology map of Kibiro (EAGER, 2018a).

Surficial geothermal features include four clusters of hot springs, inactive oil seeps, bedrock alteration, and a single weak fumarole (Figure 6B). The hottest cluster of springs ranges from 77 to 87°C and emanates from the NE end of the upper NTB fault adjacent to where it merges with the outer main NTB fault. Three other clusters of hot springs are present outboard of the main NTB fault and are aligned along a possible concealed NE-SW trending step-faults. A weakly flowing 45°C fumarole was discovered by EAGER and GRD in January of 2018 at the SW end of the step-over in an area of intense argillic bedrock alteration, native sulphur and bitumen (EAGER, 2018a). The fumarole extends the distance of surface thermal features about 750 m SW of the previously identified hot springs. Results of the previous soil CO_2 and soil temperature UNEP studies (Alexander et al., 2016) are consistent with the distribution of active thermal manifestations at either end of the double-ended step-over along the NTB fault.

To revise the conceptual model, the TEM model was combined with the updated structural mapping shown in Figure 6. The NE-SW extent of the high conductance (low average resistivity in orange to red areas) interpreted as smectite alteration in the basin-fill sediments, previously used to assess the resource extent in by Alexander et al. (2016a), aligns with the width of the step-over region along the NTB fault and the extent of the anomalous soil temperatures. The consistency between the thermodynamic implications of the geology, surficial thermal data, and TEM conductance provide increased confidence in the conceptual model. In contrast, the previous UNEP structural model (Alexander et al., 2016a) involved a single fault intersection between the NTB fault and the Kachuru fault, indicating that the upflow was possibly only along a narrow, steeply plunging fault intersection, decreasing confidence in the resource extent assessed using the TEM conductance.

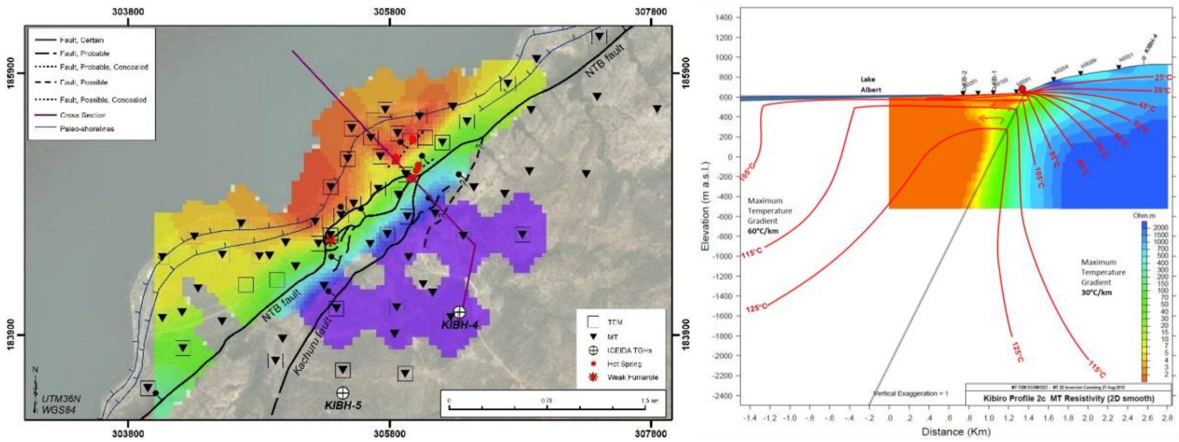

Figure 6. (A) Map of TEM conductance to 200 m depth from Alexander et al. (2016a) plotted on the new EAGER-GRD generated structural map. (B) MT 2D cross-section with conceptual model isotherms associated with upflow in fault with 65° dip and outflow into shallow gravels.

The additional data collected in 2018 support the UNEP model (Alexander et al., 2016a) with these additions: 1) higher confidence in achieving commercial production from within the NTB fault zone, and 2) equal or greater confidence in achieving commercial production from within stratigraphic-hosted outflow given higher confidence in fault-hosted up-flow, which suggests a broader area of combined fault and formation-hosted reservoir compared with the UNEP model. The main uncertainty with respect to targeting the potential outflow is the unknown permeability of the coarser basin-fill deposits and this remains unchanged by this study (a secondary risk issue is its likely lower temperature). The main risk with respect to targeting the upflow in the fault zone is the variable permeability within such fault zones.

An updated median conceptual model cross-section is presented in Figure 6B with isotherms illustrating a 125°C upflow in the NTB fault dipping 65°. Given the higher confidence that the step-over along the NTB fault provides the conduit for deep circulation, the updated conceptual model is constructed to >2000 m a.s.l. to illustrate the control that convection along this structure has on the isotherms.

4. Songwe, Tanzania

The Songwe geothermal prospect is located in western Tanzania in the Rukwa Rift of the western branch of the EARS (Figure 1). The Government of Tanzania has conducted geothermal exploration at Songwe with the assistance of external experts for the last several decades (Makundi and Kifua, 1985; Pisarskii et al., 1998; Hochstein et al., 2000; Kraml et al., 2010; and Alexander et al., 2016d). The 5 clusters of hot springs identified by these studies discharge at between about 40 and 80°C in a 3 x 1 km area near the western margin of the Songwe basin (Figure 9A). The hot spring waters are neutral to slightly alkaline (pH=6.9-8.8), low TDS (~2000-3400 mg/l) mixed Na-HCO_3-Cl-SO_4 fluids; the dominant non-condensable gas (NCG) is CO_2.

The GEOTHERM programme of the German Geological Survey (BGR) supported studies of the Ngozi-Songwe area from 2006 to 2009, including structural geology, volcanology (Delvaux et al. 2010), geophysics (Kalberkamp et al., 2010), and geochemistry of fluids and travertine deposits (Delvaux et al., 2010; Kraml et al., 2010). Structural studies of faults by

Delvaux et al. (2010) confirmed earlier observations that the faulting in the Songwe area has evolved from purely extensional to a transtensional system with both active strike-slip and normal faults. Delvaux et al. (2010) also evaluated the geochemistry of the extensive travertine deposits and acquired a U-Th age date of 360 ka from a sample at the base of one of the outcrops. Kalbercamp et al. (2010) interpreted the sparse TEM and MT data and a prominent low in the observed aeromagnetic map to indicate a resource at Ngozi that extends toward Songwe. The concluding conceptual model for the GEOTHERM studies was that Songwe Hot Springs were outflow from the volcano-hosted geothermal system at Ngozi volcano, which is located about 40 km to the ESE. Key elements of this model were that Ngozi volcano was both a potential heat source and high elevation recharge area for the Songwe geothermal system. Based on the simple conceptual model illustrated in Delvaux et al. (2010), non-buoyant outflow from Ngozi follows the topographic gradient to the west into the Songwe basin, where it discharges along a steep east-dipping normal fault along the western margin of the Songwe graben.

More recently, geoscientific analysis at Songwe was completed by TGDC supported by a team of UNEP-funded consultants (Alexander et al., 2016b). The main conclusions of the preliminary study were that Songwe is not an outflow of the neighboring Ngozi volcanic geothermal system as hypothesized in previous studies (e.g., Delvaux et al., 2010), but is instead a separate ~112°C, fault-controlled deep circulation geothermal system within the Songwe half graben in the western branch of the EARS (Alexander et al., 2016b). As shown in Figures 7A and 7B, the gravity and MT acquired and interpreted as part of the UNEP program supports a half-graben model for the Songwe basin. The reduced-to-pole aeromagnetic map prepared by the UNEP team and shown in Figure 7C indicates that the magnetic low that was correlated with geothermal alteration by Kalbermap et al. (2010) is more likely attributed to magnetic inclination distortion of a very prominent magnetic high (red in Figure 7C), interpreted by Marobhe (1989) as a carbonatite embedded in the Precambrian that is buried about 700 m, preserving its magnetite from conversion to hematite during karsting.

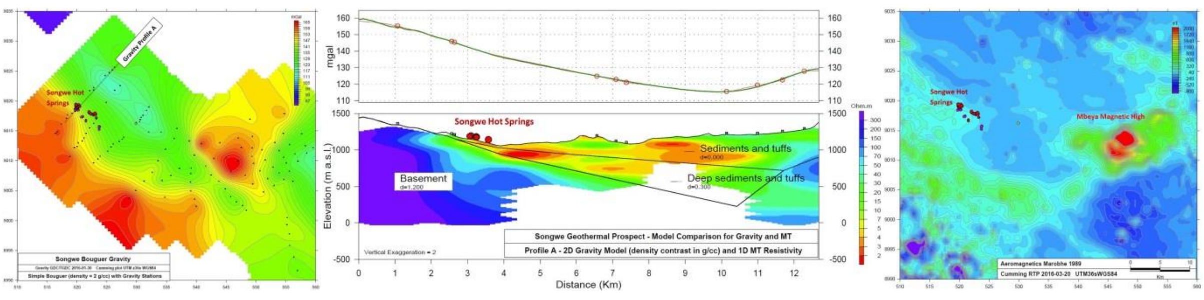

Figure 7. (A) Regional gravity of the Songwe region showing half graben with no large offset down to the NE near springs. (b) MT-gravity model along profile A. (C) Regional RTP aeromagnetic data showing partial but inconsistent correlation with Precambrian exposure.

The UNEP consultants presented two possible conceptual models, one of which was built around upflow being focused along a right step in a NE-dipping normal fault along the southwest side of Songwe basin (Figure 8A). An alternative model involves westward upflow from northeast of the Songwe hot springs through NE-dipping basin-fill sediments.

The most recent work involved detailed geologic mapping and collection of infill TEM data by EAGER and TGDC in 2018 (EAGER, 2018b). The new mapping covered 170 km^2 and produced the first comprehensive geology and structure map of the Songwe geothermal prospect area. The new maps and cross-sections (Figures 8B, 9A, B, and C) added substantial detail to the stratigraphy, fault patterns, and distribution of active and inactive surface manifestations. The most important new system of faults is the NW-striking, high angle, left-stepping, sinistral strike-slip fault system that extends through the centre of the hot springs area (Figure 8B). These faults locally cut the travertine terraces and are locally coincident with travertine fissures. In contrast to previous maps and structural models (Roberts et al., 2004; Alexander et al., 2016b), no major NE-dipping fault was identified along the NE side of the Chumwa Range. Instead, the left-stepping, NW-striking sinistral faults form a pull-apart. Pull aparts along strike-slip fault zones are one of the analog structural settings recognized in the Basin and Range region, USA (Figure 2).

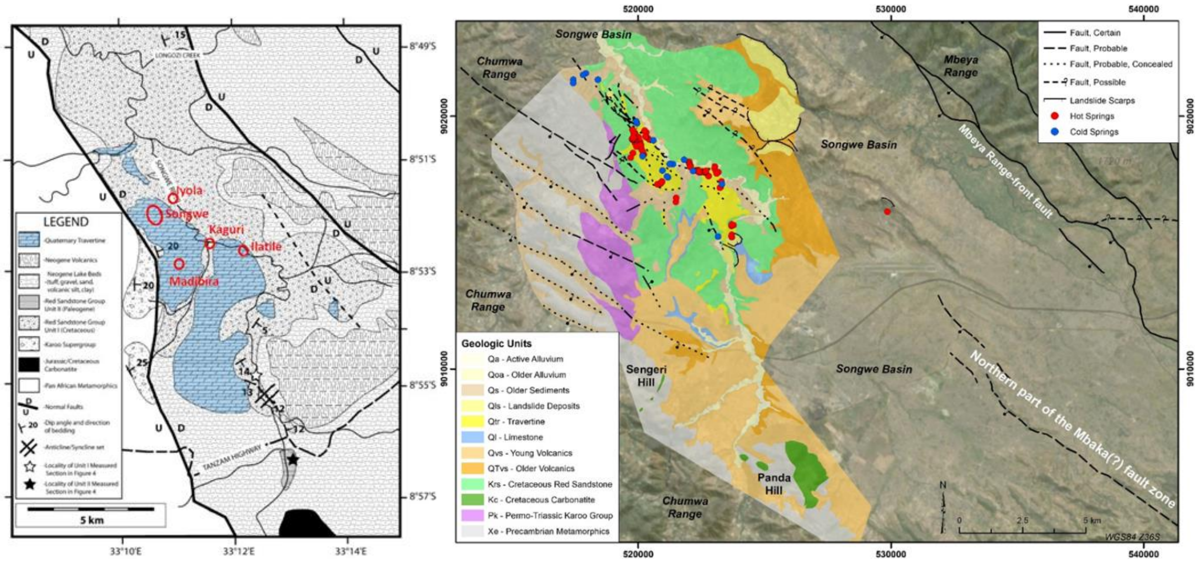

Figure 8. (A) Previous geologic map of Songwe (Alexander et al., 2016b) on the left. (B) New geologic mapping by EAGER and TGDC (EAGER, 2018b) on the right.

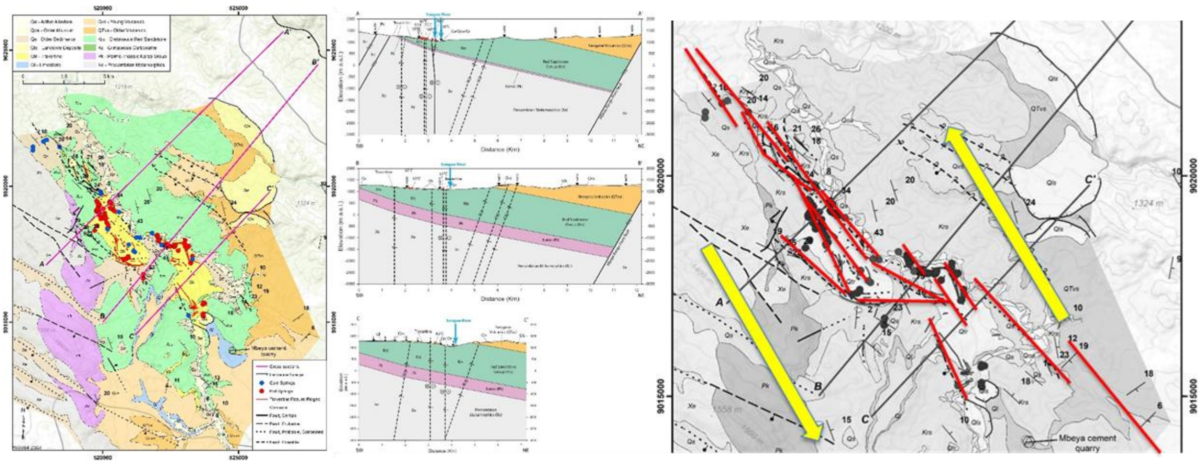

Figure 9. (A) Detail of Figure 8B. (B) Cross-sections, locations on part A. (C) On the right, a structural model for Songwe illustrating the left-stepping sinistral faults drawn on a grayscale copy of part of the map in part A. Red lines are diagrammatic faults, black dots are hot springs, and yellow arrows show sinistral fault motion.

The new mapping also identified 115 hot springs from 31 to 81°C, which is many more than the number of previously mapped springs. The distribution of hot springs covers a 10 km^2 zone that extends 5.8 km NW-SE by 1-1.75 km (Figure 10A), over double the previously mapped area. These hot springs are distributed in more than a dozen major clusters mostly aligned along travertine fissure ridges that are the loci of active extension. The artesian nature of the springs previously recognized in the UNEP study (Alexander et al., 2016b) over a 25 to 30 m range of elevation was extended in this study to 132 m elevation from 1065 m to 1197 m (Figure 9A), and travertine outcrops associated with hot springs reaching 1300 m elevation, implying a higher elevation source.

Numerous travertine fissure ridges were mapped throughout the broad extent of the travertine deposits, many of which are associated with active hot springs (Figure 9A). Overall, the travertine fissures are trending from NW to NNW, but locally, curve into the E-W trending fissures through the center of the hot springs area. Collectively these fissures form a zone 1-2 km wide, elongate NW-SE, and make a pronounced left-step. A few of the travertine fissures were found to root into the underlying Quaternary sediments and/or the Red Sandstone (EAGER, 2018b). Several of the fissures were also observed to link directly with the NW-striking strike-slip faults mapped in the Cretaceous Red Sandstone and many of the fissures are subparallel to these same faults. In addition to travertine fissures, high concentrations of calcite veins that were previously deposited by circulating geothermal fluids were also noted in parts of the Red Sandstone adjacent to the NW-striking strike-slip faults.

The new study by EAGER and TGDC is consistent with the deep-circulation model of the UNEP study but has rejected the structure and flow model emphasized in the UNEP study, which was based on a deep upflow hosted in a NE-dipping fault zone step-over along the SW side of the Songwe basin. The EAGER-sponsored geologic mapping has demonstrated that no major NE-dipping normal fault exists along this sector of the rift, a conclusion consistent with the MT and gravity data in Figure 7, which also did not resolve an offset consistent with such a fault. Unfortunately, because of coherent noise distortion by a power line detailed in EAGER (2018c), the MT resistivity profiles shown in Figures 7B and 10a, 10B and 10C have been truncated at relatively shallow depths and no 2D inversion has been reliable. Instead, the EAGER and TGDC geologic fieldwork has identified a new NW-striking system of left-stepping, left-lateral, strike-slip faults intersecting the hot springs area. This fault system is capable of facilitating deep circulation of fluids and long-lived permeability over the ~360 ka lifespan of this geothermal system.

In addition to the newly defined structural framework, the deep circulation must also be connected with one or more sources of focused downflow to maintain the observed artesian pressure, as it is unlikely for a connection by diffuse seepage to yield this magnitude of artesian pressure. There are several candidates for this recharge source, each with different implications for resource size and these, together with different types of outflow aquifers, are the principal variations considered in the conceptual model options: (1) downflow in the Chumwa Range directly southwest of the hot springs, (2) downflow in karsted carbonatite at Panda Hill, (3) isolated artesian aquifers within the strike-slip fault system, (4) downflow along the network of strike-slip faults SE of the hot springs, and (5) downflow along segments of the Mbeya Range-front fault. Of these broad conceptual model options for focused cool downflow connecting to the reservoir and yielding the artesian hot spring flow, options 4 and 5 are deemed the most likely in this study.

The simplest conceptual model is (4) downflow and upflow along-strike in the strike-slip fault zone. Presented here are pessimistic, median and optimistic thermal regimes in Figures 10A, B and C. These models are anchored toward a background conductive gradient of 30 to 35°C/km in the rock formations SW of the hot springs and slightly higher temperature gradients in the Songwe basin. The median model is based around the geothermometry estimate of 112°C within the lower part of the basin fill sediments (Figure 10A). The pessimistic (most conservative) model features a narrow upflow focused along key fault segments (Figure 10B). The shape of the isotherms is the same as the median model, except that the pessimistic model assumes lower resource temperatures. The optimistic model is an optimistic model with greater convective heat flow over the entire resource area (Figure 10C). The optimistic model also includes possible shallow outflow into the basin to the NE from the hot springs area, as indicated by the reversal in the eastward-verging 75°C isotherm in Figure 10C. Drilling TGH into such an outflow tongue at shallow depths will provide important information on the preferred model for this geothermal system.

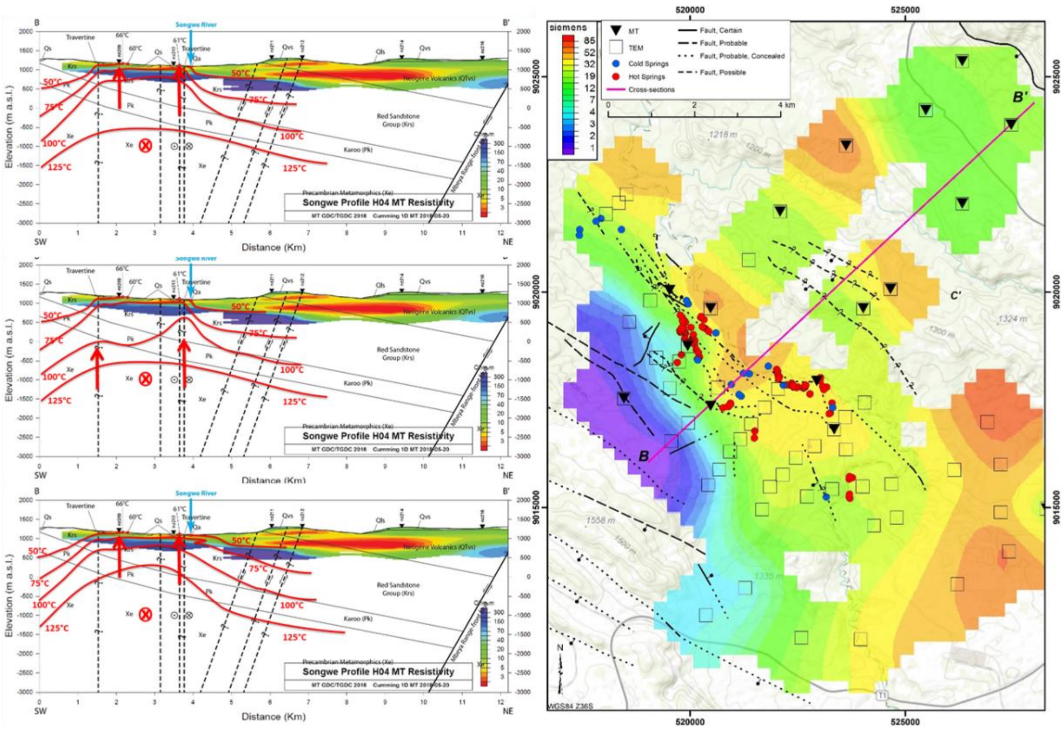

Figure 10. Model sections using Profile B-B' on right (D): (A) Upper Left, Median (B) Middle Left, Pessimistic (C) Lower Left, Optimistic. (D) Right, TEM conductance at 200m.

6. Conclusions

The EAGER program has supported detailed surface studies by GRD at the Panyimur and Kibiro geothermal prospects in Uganda and by TGDC at the Songwe geothermal prospect in Tanzania. Revised detailed structural models have been developed for each area that are comparable with analogs in the Basin and Range (e.g., Faulds and Hinz, 2015; Figure 2). These structural analyses have been decisively supported by MT and TEM resistivity surveys and gravity, reflection seismic, aeromagnetic and well log results have provided locally important constraints on the resource conceptual models.

Both Panyimur and Kibiro occupy normal fault step-overs along opposite sides of the Lake Albert basin in Uganda. In both cases the revised structural models fit the 2D MT inversions of the faulted margin and better fit the mapped MT-TEM patterns than earlier models. At Panyimur, reflection seismic across the hot springs and analyses of well logs from a nearby oil exploration well support the possibility of formation-hosted outflows of hot water toward the Lake Albert in a manner consistent with the MT and TEM.

Songwe occupies a pull-apart along a strike-slip fault system in the Songwe basin in Tanzania, a significant difference from earlier models involving a resource associated with deep-circulation in a normal fault or an outflow from the Ngozi geothermal prospect 40 km to the ESE. The revised structural model identified in the EAGER program is more consistent with the MT, TEM and gravity models, and fluid chemistry, which indicates a connection with Ngozi is very unlikely, and is in alignment with the conclusions of the 2016 UNEP study.

The EAGER geothermal exploration program updated and increased confidence in existing conceptual models for the Kibiro prospect and developed new conceptual models for the Panyimur and Songwe prospects, providing a framework for assessing resource capacity at 10%, 50% and 90% confidence levels. These models will be useful for targeting TGH wells and for guiding future exploration and development plans.

7. References

Alexander, K.B., Cumming, W., and Marini, L., 2016a, Geothermal resource assessment report: Kibiro Geothermal Prospect, Uganda: Final Report-September 2016: Confidential reported to UNEP and GRD/MEMD, 222 p.

Alexander, K., Cumming, W.B., and Marini, L., 2016b, Geothermal resource assessment report: Ngozi and Songwe Geothermal Prospects, Tanzania. Final Report dated September 2016 to UNEP/ARGeo and TGDC, 176p.

Alexander, K., Cumming, W.B., and Marini, L., 2016c, Technical Review of Geothermal Potential of Kibiro Geothermal Prospect, Uganda: Proceedings, 6th African Rift Geothermal Conference, Addis Ababa, Ethiopia, 2-4 Nov., 9 p.

Alexander, K., Cumming, W.B., and Marini, L., 2016d, Technical Review of Geothermal Potential of Ngozi and Songwe Geothermal Prospects, Tanzania: Proceedings, 6th African Rift Geothermal Conference, Addis Ababa, Ethiopia, 2-4 Nov., 11 p.

Ármannsson, H., Bahati, G., and Kato, V., 2007, Preliminary investigations of geothermal areas in Uganda, other than Katwe-Kikorongo, Buranga and Kibiro. Final Report. ICEIDA, MEMD, Uganda, 19 pp.

Ármannsson, H., 1994, Geochemical studies on three geothermal areas in West and Southwest, Uganda. Final report. Geothermal exploration UGA/92/003, UNDESD, GSMD, Uganda, 85 pp.

Árnason, K. and Gíslason, G., 2009, A summary report on a pre-feasibility study of the Kibiro and Katwe-Kikorongo geothermal prospects in Uganda, Conclusions and recommendations. Unpublished report prepared for Icelandic International Development Agency and Ministry of Energy and Mineral Development, Uganda.

Bilham, R., Bendick, R., Larson, K., Braun, J., Tesfaye, S., Mohr, P., and Asfaw, L., 1999, Secular and tidal strain across the Ethiopian rift: Geophysical Research Letters, v. 27, p. 2,789-2,984.

Delvaux, D., Kraml, M., Sierralta, M., Wittenberg, A., Mayalla, J.W., Kabaka, K., Makene, C., and GEOTHERM working group, 2010, Surface Exploration of a Viable Geothermal Resource in Mbeya Area, SW Tanzania, Part I: Geology of the Ngozi-Songwe Geothermal System: Proceedings WGC, Bali, Indonesia, Paper Number 1258, 7 p.

EAGER, 2017a, Enhanced resource modeling for Panyimur and Buranga: Confidential Report to GRD, December, 103 p.

EAGER, 2017b, Updated exploration plans for Panyimur and Buranga: Confidential Report to GRD, December, 19 p.

EAGER, 2017c, Buranga and Panyimur review and conceptual models: Confidential Presentation to GRD, December, 76 slides.

EAGER, 2018a, Review of Kibiro prospect structural geology with implications on the conceptual model and drilling program: Confidential Report to GRD, April, 25 p.

EAGER, 2018b, Enhanced resource modeling at Songwe: Confidential Report to TGDC, June, 30 p.

EAGER, 2018c, Geophysics interpretation at the Songwe Geothermal Prospect: Confidential Report to TGDC, June, 34 p.

Ebinger, C.M, and Casey, M., 2001, Continental breakup in magmatic provinces: An Ethiopian Example: Geology, v. 29, no. 6, p. 527-530.

Faulds, J.E., Bouchot, V., Moeck, I., and Oguz, K., 2009, Structural controls on geothermal systems in western Turkey: A Preliminary Report: GRC Transactions, v. 33, p. 375-381.

Faulds, N.H., and Hinz, N.H., 2015, Favorable tectonic and structural settings of geothermal settings in the Great Basin Region, western USA: Proxies for discovering blind geothermal systems: Proceedings WGC 2015, Melbourne, Australia, 6 p.

Gíslason, G., Árnason, K., and Eysteinsson, H., 2004, The Kibiro geothermal prospect, A report on a geophysical and geological survey. ICEIDA/DGSM report. GSMD, 2012, Progress report on geological investigations of Panyimur geothermal resource area, Nebbi District, 21 p.

Gislason, G., Ngobi, G., Isabirye, E., and Tumwebaze, S., 1994, An inventory of three geothermal areas in West and Southwest Uganda, UNDDSMS and GSMD report, 41 p.

Hinz, N.H., Coolbaugh, M., Faulds, J.E., Shevenell, L., and Stelling, P., 2016, Regional quantitative play fairway analysis: Methodology, global examples, and application for the East African Rift System: Proceedings, 6th African Rift Geothermal Conference, Addis Ababa, Ethiopia, 2nd – 4th November, 2016, 12 p.

IAEA, 2003, Isotope hydrology for exploring geothermal resources, UGA/8/003. IAEA TC-project UGA/8/003, Terminal report, 32 pp.

Kahwe, E., Babirye, P., Birungi, N.R., and Kabenge, L., 2013, A progressive report on geophysical investigations of Kibiro geothermal resource area, Hoima District-western Uganda. Prepared by Department of Geological Survey and Mines. Uganda Geothermal Resources Development Project 1199.

Kalberkamp, U., Schaumann, G., Ndonde, P.B., Chiragwile, S.A., Mwano, J.M., and GEOTHERM working group, 2010, Surface exploration of a viable geothermal resource in Mbeya area, SW Tanzania, Part III; Geophysics: Proceedings World Geothermal Congress, Bali, Indonesia, 6 p.

Kato, V., 2013, Geothermal exploration in Uganda status report: Short Course VIII on Exploration for Geothermal Resources, UNU-GTP, GDC, KenGen, at Lake Bogaria and Lake Naivasha, Kenya, Oct. 31 – Nov. 22, 27 p.

Keir, D., Belachew, M., Ebinger, C.J., Kendall, J.M., Hammond, J.O.S., Stuart, G.W., Ayele, A., and Rowland, J.V., 2011, Mapping the evolving strain field during continental breakup from crustal anisotropy in the Afar Depression: Nature Communications, 7 p. DOI: 10.1038/ncomms1287.

Kraml, M., Mnjokava, T.T., Mayalla, J.W., Kabaka, K., and GEOTHERM Working Group, 2010, Surface Exploration of a Viable Geothermal Resource in Mbeya Area, SW Tanzania - Part II: Geochemistry: Proceedings WGC, Bali, Indonesia, Paper Number 1455, 8 p.

Makundi, J.S. and Kifua, G.M., 1985, Geothermal features of the Mbeya prospect in Tanzania: GRC Transactions, v. 9, p. 451 - 454.

Marobhe, I.M., 1989, Interpretation of aerogeophysical anomalies of Southwestern Tanzania. Geological Survey of Finland, Bulletin 350, PhD Thesis, 78 pp.

Mawejje, P., Tunde, K. and Tamuwa, M.M., 2013, Report on geological exploration of Kibiro geothermal prospect. Prepared by Department of Geological Survey and Mines, Uganda Geothermal Resources Development Project 1199.

Morley, C., 1988, Variable extension in Lake Tanganyika: Tectonics, v. 7, p. 785-801.

Pisarskii, B.I., Konev, A.A., Levi, K.G., and Delvaux, D., 1998, Carbon dioxide-bearing alkaline hydrotherms and strontium-bearing travertines in the Songwe River valley (Tanzania): Russian Geology and Geophysics, v. 29, no. 7, p. 941-948.

Roberts, E.M., O'Connor, P.M., Gottfried, M.D., Stevens, N., Kapalima, S., and Ngasala, S., 2004, Revised stratigraphy and age of the Red Sandstone Group in the Rukwa Rift Basin, Tanzania: Cretaceous Research, v. 25, p. 749-759.

Willemson, N., van Leeuwen, W., Scheijgrond, P., 2018, Geothermal Exploration Uganda, Report on Dutch Technical Assistance for the Panyimur geothermal area. Report by MET-Support bv and IF Technology for GRD-MEMD, Uganda.